Development of first principles approach on the magnetic anisotropy in Fe/MgO interfaces

Abstract

Development of first principles approach on the magnetic anisotropy in Fe/MgO interfaces

Fe/MgO 界面における磁気異方性に関する第一原理アプローチの開発

Graduate School of
Natural Science & Technology
Kanazawa University

Division of Mathematical and Physical Sciences

Student ID: 1524012014
Name : Nurul Ikhsan
Chief Advisor : Prof. Tatsuki ODA
Date of Submission : 29 June 2018

Abstract

Fe/MgO interface remain attractive for the last decades, many interesting feature make it become kernel elements in future spintronics or magnonic devices. But underlying physical mechanisms of this multi-functional interface still remain open to be explored. We performed structural and electronic properties analysis by employing Carr-Parinello Molecular Dynamics with fully relativistic Density Functional Theory utilizing planewave basis. Investigation on large perpendicular magnetic anisotropy (PMA) in Cr-buffered Fe/MgO interface from the first-principles approach was performed. The electronic structure show that the origin of PMA come from 2-dimensional singularity of the flat band in the $\bar{X}$–$\bar{Y}$ line and $\bar{\Gamma}$–$\bar{M}$ line, this feature is proposed as the origin of the interface states, which appeared as sharp peak near Fermi level from the density of states. To observe temperature effect to the electronic structure, smearing of Fermi level in the material with metallic band was proposed. Tuning of the smearing function showed magnetic anisotropy energy (MAE) from spin orbit interaction (SOI) decrease linearly with respect to the temperature, a large change of 0.4 $\mathrm{mJ/m^2}$ observed when the temperature drops from 527K to 10.5K. Variation of the shape anisotropy by the change of temperature was included to the total MAE by considering the M(T) model introduce competition between MAE(SOI) and shape anisotropy as the temperature change.

Keywords: *Magnetic anisotropy energy, thickness dependence, temperature dependence, electric field effects, density functional theory, MRAM*

1 Introduction

In the works for the development of the devices, the family of Fe/MgO interfaces has been used as a kernel technological element. They have shown a strong perpendicular magnetic anisotropy for the thin Fe without any heavy element [1, 2]. The multi-functional properties, mentioned in the previous paragraphs, are mostly originated from the electronic structure. In such system, the interface state has been discussed in the several works [3, 4]. These states are consequences of the band formation consisting of non-bonding orbitals on the interface. Although such character has been observed as interesting characteristics, detail dependence of electric structure has not been investigated.

In the recent improvement of computational performance allows us to estimate the magnetic anisotropy or its EF effect precisely and numerically [10, 11]. Such improvement contributes not only to physical and qualitative explanations in the property of magnetic anisotropy but also to semi-quantitative agreements. In particular, the slope in the EF variation has been proved to have a realistic meaning, when compared with the experimental results [7]. On the magnetic anisotropy energy (MAE), the comparison with experiment has a distance from explaining the experimental measurements with a quantitative agreement. The experimental progress on the interface magnetic anisotropy in the thin films gives us a fascinating opportunity on a direct comparison between the theoretical and experimental approaches.

This work was devoted to the discussions on electronic, magnetic, and structural properties of Fe(x ML)/MgO(001), as a reinvestigation in the view point of two-dimensional electronic structure. We obtained remarkable Fe-thickness dependences of MAE, implying a picture of non-rigid band filling in the interface states. Such result can be discussed in terms of electronic band theory, compared with the available experimental data.

Perpendicular magnetic anisotropy (PMA) has an important role for designs of better devices of spin transfer torque recording magnetoresistive random access memory (STT-MRAM) [8, 1]. In the approaches of both theory and experiment, a lot of progress has been made for developing functionals or improving performances [7, 9, 10, 11, 12, 13, 14, 15, 16, 43]. The properties of temperature dependence in PMA are highly requested for designing ferromagnetic magnetic materials. Up to now, there are many works of theoretical approach for the systems of localized magnetic moments (single ion-magnetic anisotropies) [18, 19, 20]. In these approaches, the magnetic anisotropy energy (K) was treated as a cubic polynomial function of magnetization (M). For the metallic epitaxial films, the function of square polynomial was employed at the low temperature [21, 22]. The theoretical approaches showed that K is proportional to M^2 in case of $L1_0$-ordered FePt [23, 24] The recent density functional approach to disordered magnetic bulk alloys explains an anomalous temperature dependence of magnetocrystalline anisotropy [25].

For the design of materials in emerging nanoscale memory and logic device, Alzate *et al.* showed that in the system MgO/CoFeB/Ta-based MTJ [26], M as temperature dependence fitted well with the Blöch law ($T^{3/2}$) [27]. In addition to this, K as temperature dependence fitted well with a power law of M^2 or a similar one. Wen *et al.* also showed a similar behavior of temperature dependence on M and K in $Ru/Co_2FeAl/MgO$-based MTJ [28]. For the thinner films of several iron monolayers, the temperature dependence of M was implied to change from $T^{3/2}$ to T^2 [33].

In the materials for perpendicular-MRAM devices, the property of PMA is mainly ascribed to spin-orbit coupling (SOC) in the metallic electronic structure. The magnetocrystalline anisotropy for metal has been estimated successfully since the 1980's using density functional approaches. The PMA of thin films has qualitatively or semi-quantitatively been explained. This is a consequence of the fact that the PMA from SOC overcomes the magnetic shape anisotropy (SA) which favors in-plane magnetization. The latter contribution to magnetic anisotropy has been investigated for a long time, including its temperature-dependent property. However, the temperature dependence of the magnetic anisotropy caused by metallic energy bands has not been investigated very well, particularly for thin film systems.

In the present work, we investigated smearing effects on the Fermi level in terms of the magnetic anisotropy energy of the metal slab system for magnetic devices, employing a first-principles calculation. These effects are expected to contribute to a temperature dependence on the magnetic anisotropy caused by SOC. In combination with SA analyses, a saturating behavior in K at room temperatures may be comprehended, compared with the available experimental data [15].

2 Method

Density functional theory (DFT) code based on Carr-Parinello molecular dynamics has been used to perform simulation in this research. The CPVO codes [29] is built based on plane wave basis, by utilizing the ultrasoft pseudopotential and generalized gradient approximation in the exchange correlation term the many body electron problem were solved. The structural optimization is performed in scalar relativistic

calculation, but finally we calculate the magnetic anisotropy energy by using full relativistic calculation, with considering spin orbit interaction.

The MAE originating from spin-orbit interaction (SOI) was estimated from the total energy difference between the different magnetization directions [100] (x-axis) and [001] (z-axis), MAE(SOI) = E[100] − E[001], where [001] specifies the direction of film thickness. We used the 32 × 32 × 1 mesh of **k** point sampling [30] in MAE estimation [37]. Using the scalar-relativistic level computation, in which taking a 24 × 24 × 1 **k**-mesh, we induced structural relaxation while keeping both the in-plane lattice constant and the atomic coordinates of O(3). The MAE from the shape anisotropy, MAE(MDI), was estimated using the magnetostatic dipole interaction (MDI) and assuming the atomic magnetic moments

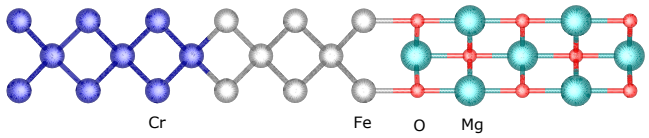

Figure 1: Schematic model of the slab systems Cr(6ML)/Fe(xML)/MgO(5ML) for $x = 5$.

To investigate the interface of Fe/MgO, we consider slab model consisting 0.79 nm vacuum. The construction is vacuum/Cr(6 ML)/Fe (x ML)/MgO (5 ML)/vacuum, ML means atomic monolayer. This structure are illustrated in Fig. 1. We build our computational model based on the slab model for metal. Every atom stacked in pillar-like position with two large vacuum at the both end of the model. So it has infinite 2-dimensional boundary, but with finite z-direction thickness.

In this work the thickness of Cr is already fixed to 6 ML because it has been known from previous work[32], that the thickness of buffer layer is does not effect to the estimation of MAE. 6 ML configuration assumed to be enough, also in this model we could build antiferromagnetic configuration for the Cr underlayer. Previous works show, MAE is almost independent of Cr thickness within the accuracy of 0.1mJ/m^2 for a given Fe thickness.

To understand the **k**-space contributions to the MAE, the **k**-resolved MAE, defined as MAE(**k**) = $\sum_n (f_{n\mathbf{k}}^{[100]}\varepsilon_{n\mathbf{k}}^{[100]} - f_{n\mathbf{k}}^{[001]}\varepsilon_{n\mathbf{k}}^{[001]})$ + (correction term), was calculated, where the correction term above was assumed to be a uniform in **k**-space and the integrated value of MAE(**k**) is equal to the MAE(SOI). After excluding the trivial contribution which is cancelled out with each other by symmetrizing MAE(**k**).

The magnetic anisotropy also depends on the magnetic moment. As temperature of the magnetic moment decreases, the anisotropy energy often becomes decreased. The main part of such reduction may be realized by the contribution of SA. The temperature dependence of the magnetic moment originates from the spin fluctuations. In order to evaluate it, one can take a method based on the microscopic electronic structure [23, 24]. However, for focusing the smearing effect at the Fermi level and for simplicity, this work employs a well-known sophisticated model as the temperature-dependent magnetization $M(T)$, as follows: $M(T) = M_0\, y(T/T^*)$, where y is a given function, $M_0 = M(0)$, and T^* is a sophisticated parameter, such as Curie temperature (T_c). T^* is used as a sort of fitting parameters. In this work, due to the thinner magnetic slab, we employed $y(T/T^*) = 1 - (T/T^*)^2$ [33].

The magnetic anisotropy energy is presented as $K = K_b + K_{sa}$, where K_b is from the band energy and K_{sa} from the SA. K_b is expressed as the energy difference of free energy F_b between the different magnetization directions, such as [100](x-direction) and [001](z-direction). The F_b is given as follows [34, 35] :

$$F_b = \sum_{n\mathbf{k}} f_{n\mathbf{k}}\,(\varepsilon_{n\mathbf{k}} - \mu) - k_B T S + E_d + \mu N_e\,, \tag{2.1}$$

where E_d is the double counting term in the total energy.[36] Using Eq. (2.1), $K_b = F_b^{[100]} - F_b^{[001]}$ [37]. The K_{sa} is expressed as $K_{sa} = -\mu_0 M^2/2\Omega + \Delta K_{sa}^{int}$, where Ω and μ_0 are the volume of magnetic slab and permeability of vacuum, respectively, and ΔK_{sa}^{int} is the interface contribution which does not include in the 1st term. ΔK_{sa}^{int} originates from both the discreetness of stacking atomic layers [38] and the deviation from spherical atomic spin moment density at the interface magnetic atoms [39]. These are due to the shape of magnetization distribution, reducing the in-plane SA in ferromagnetic Fe layers.

In the demonstration, we used the slab system, vacuum(0.79nm)/Cr(6ML)/Fe(5ML) /MgO(5ML)/vacuum(0.79nm) (ML=atomic monolayer). At the Fe/MgO interface the Fe atom was placed just next to the O atom due to its stability, and in the Cr and Fe layers the body-centered layer-stacking sequence was used. The in-plane lattice constant extracted from bulk Cr was employed.

The density functional calculation employs a fully relativistic (with spin-orbit interaction) ultrasoft pseudopotentials and planewave basis [40], by using the generalized gradient approximation [41]. We

used a $32 \times 32 \times 1$ (sparse) mesh for the $\mathbf{k}$ point sampling in the estimations of K_b. At the low temperatures, unfortunately, the sparse mesh mentioned above cannot give any convergence in the self-consistent calculation, and a $64 \times 64 \times 1$ (dense) mesh was also introduced. The difference from the sparse mesh appeared at the low temperatures, such as less than or equal to 100-200 K, and becomes small at 300 K. The dense mesh requires a large amount of computational source so that the number of calculated temperature points were limited to a few.

3 Result and Discussion

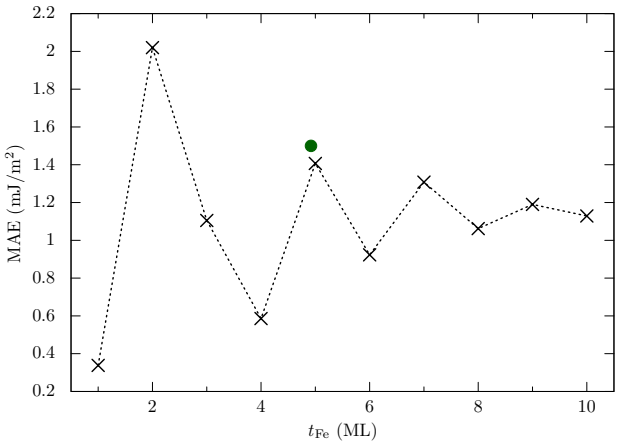

Figure 2: Thickness dependence of the magnetic anisotropy energy (MAE) from spin-orbit interaction in Cr/Fe(xML)/MgO. The bullet indicates the experimental value (ref. [43]), where 1ML thickness is assumed to be 0.142 nm.

We report the thickness dependence of MAE(SOI) in Fig. 2. The maximum MAE at Fe 2ML is much larger than the previous theoretical and experimental values in the Fe/MgO interface family, comparable to the interface contribution extracted from the extrapolation fitting in the experiment [16]. At Fe 5ML our value agrees well with the experimental value [43]. It indicates an oscillating perpendicular anisotropy with respect to Fe thickness (x), and the maximum of 2.0 mJ/m^2 at Fe 2ML($x = 2$) and other maximal values at 5ML($x = 5$) and 7ML($x = 7$). The behavior shows that an odd-even alternating oscillation at the thicker systems (4ML-10ML). For the thinner systems, the amplitude of oscillation is largely enhanced since large changes are expected in the electronic structure around the Fe/MgO interface.

Fig. 3 shows the projected density of states (PDOS) at the interface in $x = 2$ and band dispersions with $3d$ orbital components in the vicinity of the Fermi level (E_F). As shown, the E_F is located between the two peaks of PDOS consisting of $3d$ orbitals. These electronic states are relatively localized since the main orbital components are made of the non-bonding $3d$-orbitals. Indeed, the states form a flat band around the $\mathbf{k}$-point $\mathbf{k}_1 = \pi/a(1/2, 1/2)$ (see Fig. 3) and a saddle point near $\mathbf{k}_1$ in two-dimensional Brillouin zone (2DBZ). The band flatness appears along $\bar{\mathrm{X}}$–$\bar{\mathrm{Y}}$ line in 2DBZ. These features are remarkably observed for both the occupied and unoccupied bands in Fig. 3(c). There is a saddle point nature around $\mathbf{k}_1$ in 2DBZ (not exact of saddle point). Along $\bar{\mathrm{X}}$–$\bar{\mathrm{Y}}$, there is a maximum at $\mathbf{k}_1$ in the $3d$-orbital band just above E_F, and simultaneously along $\bar{\Gamma}$–$\bar{\mathrm{M}}$ a minimum near $\mathbf{k}_1$.

This feature is the origins of sharp PDOS peaks in the interface states, appearing more or less in the Fe/MgO and its family systems. However, for realizing such features, there may be a combination of two conditions. The one is an appropriate orbital hybridization between 1st Fe and 2nd Fe layers. This keeps splitting the mixed eigenstates of d_{xz} and d_{yz} components at $\bar{\mathrm{M}}$ point to the lower and higher eigen energies, while in the Fe 1ML system, those stays remain on or around E_F [49]. The 2nd condition is also an orbital hybridization between Fe $d_{3z^2-r^2}$ and O p_z. This keeps the $d_{3z^2-r^2}$ away from E_F, not disturbing the localized states of non-bonding d_{xy}, $d_{x^2-y^2}$, d_{xz}, and d_{yz} at E_F. The latter has been well known as one of important origins for realizing perpendicular anisotropy [2]. This is because the orbital $d_{3z^2-r^2}$ always contributes only to in-plane magnetic anisotropy, assuming that the contribution from the majority spin state can be neglected due to a large exchange splitting [49]. The MAE maximum in Fe 2ML is obtained as the consequences of the origins discussed above. Note that there are vertical couplings of SOI around $\mathbf{k}_1$ area in 2DBZ, which contribute to perpendicular anisotropy; couplings of d_{xy}–$d_{x^2-y^2}$ and d_{xz}–d_{yz}.

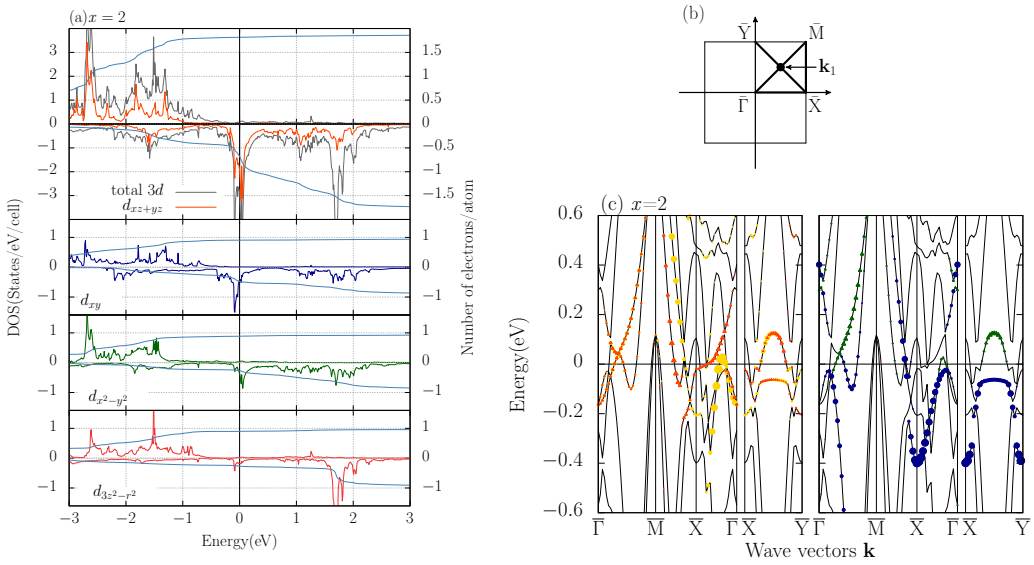

Figure 3: Electronic structures at the Fermi level in Cr/Fe(2ML)/MgO without including spin-orbit interaction, (a) projected densities of states (PDOS)(form the top) 3d total d_{xz+yz}, d_{xy}, $d_{x^2-y^2}$,$d_{3z^2-r^2}$ components, (b) selected **k**-point path, and (c) band dispersion for the Fe $3d$ orbitals at the interface Fe(1)

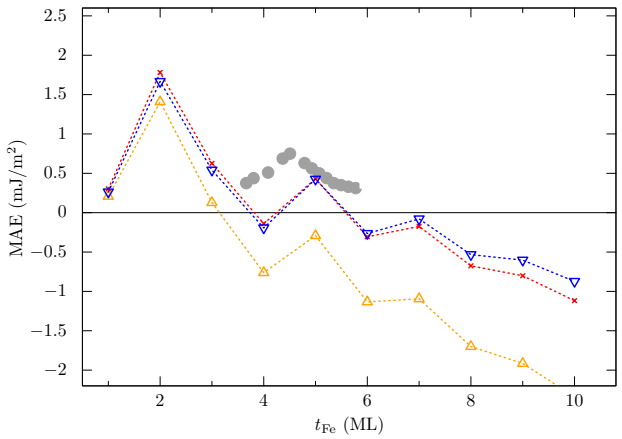

Figure 4: Total magnetic anisotropy energy (MAE), compared with the experimental data (bullets)(ref. [16]). The open yellow triangle symbol specifies the data estimated theoretically; MAE(SOI)+MAE(MDI), the reverse blue triangle symbol represent the MAE(SOI+MDI) after the 26% reduction of theoretical atomic moment, and the cross data the sum of the theoretical MAE(SOI) and the shape anisotropy MAE(SA) estimated using the experimental magnetization.

Fig. 4 reports the total MAE, namely summation of MAE(SOI) and MAE(SA), in comparison with the available experimental data. This figure shows that our estimation is much reduced due to large in-plane contribution from the MDI. As shown in Fig. **??**, the experimental MAE(SA) is much reduced in absolute, compared with the theoretical one. This is an origin why we have so much reduced value. By considering the reduced MDI (rMDI), we could obtain that the MAE (SOI+rMDI) describe in the blue reverse triangle. In this result we could observe an agreement with the experimental data [16].

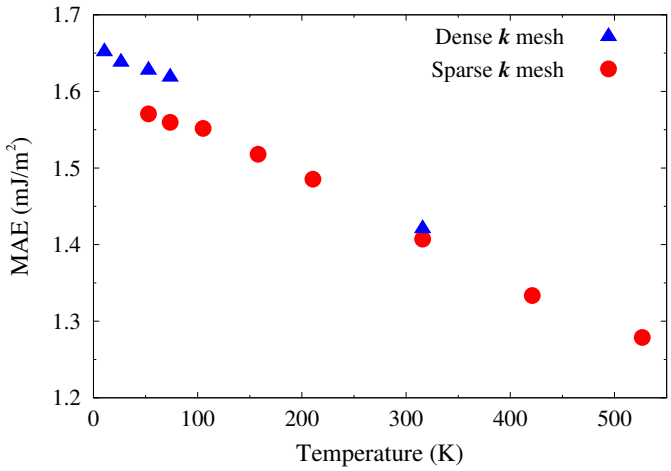

Figure 5: Fermi level smearing effect in magnetic anisotropy energy (MAE) with respect to temperature. The symbols of triangle and circle specify the data by dense and sparse meshes, respectively.

Fig. 5(b) shows $K_{\rm b}$ per unit area as a function of T. These values are positive, contributing to a perpendicular magnetic anisotropy as expected in a family of Fe/MgO interfaces [1, 7, 2], and similar to the data (1.5 mJ/m^2) from the experimental measurement at the room temperature for the Fe thickness ($t_{\rm Fe}$) of 0.7nm [43]. Such positive contribution may be attributed to the SOCs between the orbital components of d_{xy} and $d_{x^2-y^2}$, or d_{xz} and d_{yz} in the respective occupied and unoccupied states [42]. The smearing effect decreases $K_{\rm b}$ monotonically by 0.38 mJ/m^2 from 10.5 K to 527 K. This decreasing quantity is not negligible, implying one of important ingredients for the temperature dependence of magnetic anisotropy.

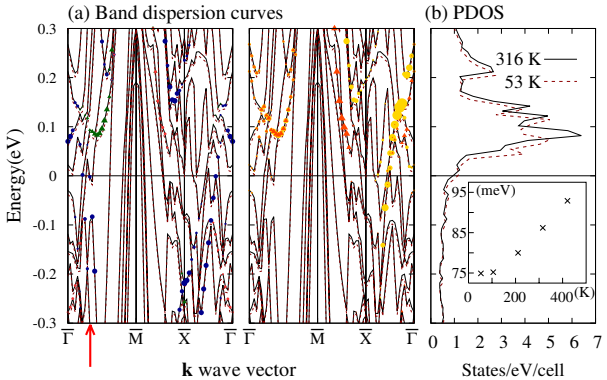

Figure 6: (a) Band dispersion curves (left and center) and (b) partial density of states (right) for the minority-spin-state 3d orbital on the interface Fe in the [001] magnetization system determined with the temperature-dependent Fermi level smearings of 316 K (full curves and symbols) and 53 K (broken curves). The symbols specify the angular orbital components projected on the interface Fe atoms; $d_{xy}, d_{x^2-y^2}, d_{3z^2-r^2}$(left) in blue, green, and red bullets, respectively, and d_{xz}, d_{yz} (center) in orange and yellow. The Fermi levels are adjusted to zero in the vertical axis with the horizontal full line, and the Fermi energy (chemical potential μ) decreases by 0.11 eV as temperature. The inset figure in (b) shows the typical data of $\varepsilon_{n\mathbf{k}} - \mu$ with respect to the temperature at $\mathbf{k} = 0.33 \times \bar{\Gamma}\bar{\rm M}$ (vertical red arrow).

$K_{\rm b}$ decreasing with temperature is a consequence of electronic structure. To confirm the variation

property, in Fig. 6 we show the band dispersion curves and the partial density of states (PDOS) for two different temperatures (53 K and 316 K). The eigenvalue with respect to the chemical potential ($\varepsilon_{n\mathbf{k}}-\mu$) is increased roughly by 0.01 eV in almost all the Brillouin zone. In particular, focusing the unoccupied states dominated by 3d orbitals at around 0.09 eV, the eigenvalue tends to behave $(\varepsilon_{n\mathbf{k}}-\mu)=\varepsilon^0_{n\mathbf{k}}-\mu_0+\alpha T^2$, where $\varepsilon^0_{n\mathbf{k}}$ and μ_0 are the eigenvalue and chemical potential, respectively, extrapolated to 0 K, and α is a positive constant (typical temperature dependence of $\varepsilon_{n\mathbf{k}}-\mu$ is shown in the inset of Fig. 6). Consequently, the quantity of $1/(\varepsilon_{n\mathbf{k}}-\mu)$ decreases as temperature, implying a decrease in K_b considering the second-order perturbation formula for spin-orbit interaction [42]. In the present case, the α is small so that $\alpha T^2/(\varepsilon^0_{n\mathbf{k}}-\mu_0)$ is much smaller than unity, showing a gradual temperature dependence in K_b like a linear, instead of a complicated dependence. Quantitatively the decreasing rate by the Fermi level smearing should be canceled out partially by the other contributions so as to showing a gradual decline such as observed in the experimental measurement [15].

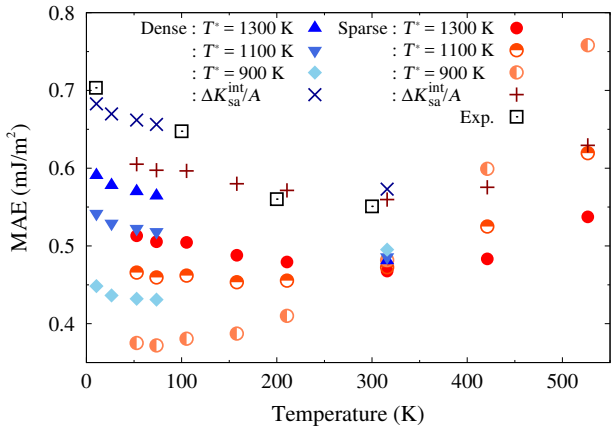

Figure 7: Total magnetic anisotropy energy (K) per unit area with respect to temperature. The symboles of triangle, bullet, circle, diamond indicate the data of $T^*=900, 1100, 1300$K for $\Delta K^{\mathrm{int}}_{\mathrm{sa}}=0$ and those of cross and plus for $T^*=1300$K and $\Delta K^{\mathrm{int}}_{\mathrm{sa}}/A=0.09\mathrm{mJ/m^2}$, where A is the interface area. The empty square symbols specify the experimental data extracted from reference [15].

In order to validate the smearing effects obtained above comparing them with the experimental results, we had performed a simulation on K using the parameters of M_0 and T^*. In this simulation we used the Fe layer thickness ($t_{\mathrm{Fe}}=0.710$nm). This t_{Fe} is comparable to those obtained by the first-principles calculation. As a result the M_0 can be fixed to the value which reproduces the experimental magnetization at 300 K ($M(300\mathrm{K})=1.83$ T) [16]. We also found that, comparing the results of the T^*s of 800, 900, 1000, 1100, 1200, 1300, and 1400K, the T^*s between 1200K and 1300K give a reasonable fitting to the temperature dependence of available experimental data [15] except a temperature-independent value implying $\Delta K^{\mathrm{int}}_{\mathrm{sa}}$. In Fig. 7, the total K per area are plotted as temperature for the parameters of $T^*=$ 900K, 1100K, and 1300K, where $\Delta K^{\mathrm{int}}_{\mathrm{sa}}=0$. At the lower T^*s, the in-plane SA becomes larger and the difference with the experimental data also becomes large at the low temperatures.

In Fig. 7, the total K per unit area is also shown for a non-zero $\Delta K^{\mathrm{int}}_{\mathrm{sa}}$. This plot implies that, assuming the interface contribution of SA ($\Delta K^{\mathrm{int}}_{\mathrm{sa}}/A=0.09\mathrm{mJ/m^2}$), K becomes close to the experimental results. This quantitative assumption in $\Delta K^{\mathrm{int}}_{\mathrm{sa}}$ is not so far from a realistic contribution, because the quadrupole atomic spin density of prolate type at the interface can reduce the in-plane SA by an energy comparable to that in the free-standing Fe 1ML (0.10mJ/m^2) [39]. Note that such contribution does not depend on the total magnetization. On the fitting to another experimental data of $M(300\mathrm{K})=2.09$T,[43] the set of parameters ($\Delta K^{\mathrm{int}}_{\mathrm{sa}}/A=0.35\mathrm{mJ/m^2}$, $T^*=1400$K) provides a reasonable temperature dependence in K. This parameter of $\Delta K^{\mathrm{int}}_{\mathrm{sa}}$ is not too large, because the parameter originates from both interfaces in the Fe layer. Further investigations on the origin of $\Delta K^{\mathrm{int}}_{\mathrm{sa}}$ are required for analyzing real magnetic interfaces.

In the case of consideration when we decrease the thickness of Fe layer, for example become 2ML, the ferromagnetic state may become unstable against thermal disturbance. This could be denied in a discussion of Cr–Fe magnetic interaction. The Fe at the Cr/Fe interface has a strong antiferromagnetic interaction of Heisenberg type. This stabilizes the ferromagnetic state of Fe thin layer. The previous works reported large exchange interactions of $J=69$ meV and $|J|$=59, 20 meV for Fe-Fe and Cr-Fe nearest neighbors, [44, 45, 46] respectively. They could be enough to maintain the ferromagnetic states at room temperatures. However, practically, associated with the existence of magnetic dead layer in such

system, [16] Fe atom may diffuse into the Cr layer during the fabricating process at high temperatures. Indeed, when exchanging the Fe and Cr atoms at the Cr/Fe interface in Fe 4ML, the total energy does not become so higher (50 meV/in-plane Fe).

As shown in Figs. 3 the interface state discussed here is presented just as some sharp peaks in this work. The main body of states is on $E_{\rm F}$ or just above $E_{\rm F}$ by less than 0.2 eV. These energy levels are located at the same energy range in which the enhanced magnetic tunneling spectra appears [43]. The interface states in the present work may have the potential to make a state resonating with the conduction electron through the $s-d$ interaction at the interface [47]. Indeed, the enhanced spectra in the spin-dependent tunnel conductance has been observed, implying some unknown/non-resolved mechanism behind [48, 3].

The Fe layer, forming a quantum well structure, is terminated at the Fe/MgO and Cr/Fe interfaces, calling the amplitudes of wave function at the edges have a feature of odd-even alternating behavior in the one dimensional model chain of which the atomic site is connected with electron transfer integral. The d_{xy} component at the Fe/MgO interface is largely affected due to its non-bonding nature, and can be sensitive to external perturbation from the other edge of Cr/Fe interface. The electron transfer between the d_{xy} orbitals of neighboring Fe MLs is proportional to $T_{xy,xy}(\mathbf{k}) \sim e^{i\mathbf{k}\cdot\mathbf{R}}\{3t(dd\sigma) + 2t(dd\pi) + 4t(dd\delta)\}/9$, and is not negligible because the absolute of transfer integral can reach to about 0.1 eV [49]. Consequently, as an edge effect of the model chain, some non-negligible changes of d_{xy} are supposed to appear at the interface states.

4 Summary

Systematic investigation on Cr-buffered Fe/MgO interface has been performed in this work. Starting from the change in thickness of ferromagnet layer, until the temperature dependence by the change of Fermi level smearing. We performed first principles electronic structure calculations for the interface systems with Cr underlayer of Fe/MgO interface and estimated the MAE originating from the SOI and MDI. The exotic oscillating behavior was observed in the MAE from SOI. We found that the DFT approach can describe the MAE with good accuracy, compared with the experimental data. Our calculation shows that the MAE(SOI) in 5ML system with 1.5 mJ/m^2 is comparable to the experimental ones. The series of total MAE's indicated perpendicular and in-plane magnetic anisotropies in the Cr-underlayer Fe/MgO. The reduction by the in-plane shape anisotropy energy was considered as the correction factor to the pure DFT calculation approach. By introducing the rescaled magnetization similar to the experimental one, the thickness range of perpendicular magnetic anisotropy was found to correspond to experimental result. From the electronic structure, the dispersionless and saddle point nature appear in the band dispersions around $\mathbf{k}_1$ are found to play the important role in the perpendicular anisotropy. In the Fe 2ML, particularly, the flat bands consisting of d_{xz}, d_{yz}, d_{xy}, $d_{x^2-y^2}$ are located just below and above the Fermi level. These bands contribute to the large MAE(SOI) of 2 mJ/m^2. The change of interface states as an effect of vicinity of Cr under-layer and the formation of quantum-well is discussed as the origin of change in perpendicular magnetic anisotropy like a proximity effect. The detail electronic and magnetic properties of this Cr buffered Fe/MgO slab systems, might be useful in future materials design for such multi-functional interfaces.

We performed the first-principles calculations on the MAE from the band energy contribution using the temperature-dependent Fermi level smearing in the Fe(5ML)/MgO slab. The contribution of the MAE decreases by 0.4 mJ/m^2 as temperature from 10.5K to 527K. When employing the simple formula for the SA and assuming the experimental saturated magnetization with the appropriate temperature dependence for ultra-thin films, the total MAE shows a nearly flat part around the room temperature.

References

[1] S. Ikeda, K. Miura, H. Yamamoto, K. Mizunuma, H. D. Gan, M. Endo, S. Kanai, J. Hayakawa, F. Matsukura, and H. Ohno, Nat. Mater. **9** , 721 (2010).

[2] R. Shimabukuro, K. Nakamura, T. Akiyama, and T. Ito, Physica E **42**, 1014 (2010).

[3] P.-J. Zermatten, G. Gaudin, G. Maris, M. Miron, A. Schuhl, C. Tiusan, F. Greullet, and M. Hehn, Phys. Rev. B, **78** 033301 (2008).

[4] I. Rungger, O. Mryasov, and S. Sanvito, Phys. Rev. B **79**, 094414 (2009).

[5] C.-G. Duan, J. P. Velev, R. F. Sabirianov, Z. Zhu, J. Chu, S. S. Jaswal, and E. Y. Tsymbal, Phys. Rev. Lett. **101**, 137201 (2008).

[6] K. Nakamura, R. Shimabukuro, Yuji Fujiwara, T. Akiyama, T. Ito, and A. J. Freeman, Phys. Rev. Lett. **102**, 187201 (2009).

[7] T. Nozaki, Y. Shiota, M. Shiraishi, T. Shinjo, and Y. Suzuki, Appl. Phys. Lett. **96**, 022506 (2010).

[8] H. Ohno, Nat. Mater. **9**, 952 (2010).

[9] M. Endo, S. Kanai, S. Ikeda, F. Matsukura, and H. Ohno, Appl. Phys. Lett. **96**, 212503 (2010).

[10] C. G. Duan, J. P. Velev, R. F. Sabirianov, Z. Zhu, J. Chu, S. S. Jaswal, and E. Y. Tsymbal, Phys. Rev. Lett. **101**, 137201 (2008).

[11] K. Nakamura, R. Shimabukuro, Y. Fujiwara, T. Akiyama, T. Ito, and A. J. Freeman, Phys. Rev. Lett. **102**, 187201 (2009).

[12] T. Maruyama, Y. Shiota, T. Nozaki, K. Ohta, N. Toda, M. Mizuguchi, A. A. Tulapurkar, T. Shinjo, M. Shiraishi, S. Mizukami, Y. Ando, and Y. Suzuki, Nat. Nanotechnol. **4**, 158 (2009).

[13] Y. Shiota, T. Nozaki, F. Bonell, S. Murakami, T. Shinjo, and Y. Suzuki, Nat. Mater. **11**, 39 (2012).

[14] Y. Hibino, T. Koyama, A. Obinata, T. Hirai, S. Ota, K. Miwa, S. Ono, F. Matsukura, H. Ohno, and D. Chiba, Appl. Phys. Lett. **109**, 082403 (2016).

[15] Q. Xiang, Z. Wen, H. Sukegawa, S. Kasai, T. Seki, T. Kubota, K. Takanashi and S. Mitani, J. Phys. D: Appl. Phys. **50**, 40LT04 (2017).

[16] T. Nozaki, A. Kozio-Rachwa, W. Skowroski, V. Zayets, Y. Shiota, S. Tamaru, H. Kubota, A. Fukushima, S. Yuasa, and Y. Suzuki: Phys. Rev. Appl. **5**, 044006 (2016).

[17] J. W. Koo, H. Sukegawa, S. Kasai, Z. C. Wen, and S. Mitani, J. Phys. D: Appl. Phys. **47**, 322001 (2014).

[18] J. Kanamori, "Anisotropy and Magnetostriction of Ferromagnetic and Antiferromagnetic Materials", in Magnetism Volume 1 (H. Suhl and G. T. Rado, Academic Press, New York, 1963) Chap. 4, p. 127.

[19] E. R. Callen and H. B. Callen, J. Phys. Chem. Solids **27**, 1271 (1966).

[20] Y. Millev and M. Fähnle, Phys. Rev. B, **52**, 4336 (1995).

[21] J.-U. Thiele, K. R. Coffey, M. F. Toney, J. A. Hedstrom, and A. J. Kellock, J. Appl. Phys. **91**, 6595 (2002).

[22] S. Okamoto, N. Kikuchi, O. Kitakami, T. Miyazaki, Y. Shimada, and K. Fukamichi, Phys. Rev. B **66**, 24413 (2002).

[23] O. N. Mryasov, U. Nowak, K. Y. Guslienko, and R. W. Chantrell, Europhys. Lett. **69** 805 (2005).

[24] J. B. Staunton, S. Ostanin, S. S. A. Razee, B. L. Gyorffy, L. Szunyogh, B. Ginatempo, and E. Bruno, Phys. Rev. Lett. **93**, 257204 (2004).

[25] I. A. Zhuravlev, V. P. Antropov, and K. D. Belashchenko, Phys. Rev. Lett. **115**, 217201 (2015).

[26] J. G. Alzate, P. K. Amiri, G. Yu, P. Upadhyaya, J. A. Katine, J. Langer, Appl. Phys. Lett. **104**, 112410 (2014).

[27] F. Bloch, Z. Phys. **61**, 10.1007 (1930).

[28] Z. Wen, H. Sukegawa, T. Seki, T. Kubota, K. Takanashi, and S. Mitani, Sci. Rep. **7**, 45026 (2017).

[29] http://cphys.s.kanazawa-u.ac.jp/ oda/user-man-eng/

[30] H. J. Monkhost and J. D. Pack, Phys. Rev. B **13**, 5188 (1976).

[31] M. Tsujikawa, A. Hosokawa, and T. Oda, Phys. Rev. B **77**, 054413 (2008).

[32] N. Ikhsan, T. Kanagawa, I. Pardede, D. Yoshikawa, T. Oda, Submitted, (2018).

[33] U. Köbler, J. Phys.: Condens. Mater **14**, 8861 (2002).

[34] M. Weinert and J. W. Davenport, Phys. Rev. B **45**, 13709 (1992).

[35] T. Oda, J. Phys. Soc. Jpn, **71**, 519 (2002).

[36] G. H. O. Daalderop, P. J. Kelly, M. F. H. Schuurmans, and F. Jansen, Phys. Rev. B **41**, 11919 (1990).

[37] M. Tsujikawa, A. Hosokawa and T. Oda, Phys. Rev. B **77**, 054413, (2008).

[38] H. J. G. Draaisma and W. J. M. de Jonge, J. Appl. Phys. **64**, 3610 (1988).

[39] T. Oda and M. Obata, J. Phys. Soc. Jpn, **87**, 064803 (2018).

[40] T. Oda and A. Hosokawa, Phys. Rev. B **72**, 224428 (2005).

[41] J. P. Perdew, J. A. Chevary, S. H. Vosko, K. A. Jackson, M. R. Pederson, D. J. Singh, and C. Fiolhais, Phys. Rev. B **46**, 6671 (1992).

[42] D.-S. Wang, R. Wu, and A. J. Freeman, Phys. Rev. B **48**, 15886 (1993).

[43] J. W. Koo, H. Sukegawa, S. Kasai, Z. C. Wen, and S. Mitani, J. Phys. D: Appl. Phys. **47**, 322001 (2014).

[44] M. Yu. Lavrentiev, R. Soulairol, Chu-Chun Fu, D. Nguyen-Manh, and S. L. Dudarev, Phys. Rev. B **84**, 144203 (2011).

[45] H. Hasegawa, Phys. Rev. B., **42**, 2368 (1990).

[46] M. Ogura, H. Akai, and J. Kanamori, J. Phys. Soc. Jpn. **80**, 104711 (2011).

[47] J. M. Ziman, *Principles of the theory of solids*, (Cambridge University Press, Cambridge, 1972), p. 343.

[48] Y. Ando, T. Miyakoshi, M. Oogane, T. Miyazaki, H. Kubota, K. Ando, and S. Yuasa, Appl. Phys. Lett. **87**, 142502 (2005).

[49] D. S. Wang, R. Wu, and A. J. Freeman, Phys. Rev. B **47**, 14932 (1993).

平成３０年　８月　６日

学位論文審査報告書（甲）

１．学位論文題目（外国語の場合は和訳を付けること。）

Development of first principles approach on the magnetic anisotropy in Fe/MgO interfaces

（和訳：Fe/MgO 界面における磁気異方性に関する第一原理アプローチの開発）

２．論文提出者　(1) 所　　属　　数物科学　　専攻

(2) 氏（ふり）　名（がな）　Nurul（ぬるる） Ikhsan（いくさん）

３．審査結果の要旨（600～650 字）

Nurul Ikhsan 氏の提出論文について，各審査委員が個別に検討し，予備審査会の後，詳細に検討した。平成３０年８月３日に開催された公聴会(口頭発表)の後に，審査委員会を開催し，協議の結果以下のように判定した。

Ikhsan 氏は，密度汎関数法に基づいた第一原理電子状態計算(非経験的電子構造計算)を用いて，面直磁気異方性を示し Fe/MgO 界面をもつ薄膜系の磁気異方性エネルギー(MAE: Magnetic Anisotropy Energy)を評価した。MAE を非経験的理論計算から高精度に評価することは，計算物質科学分野において困難な問題とされる。彼は大型計算機を駆使し，電界駆動型磁気記憶素子の記憶層材料の磁性薄膜に対して，MAE の評価を行うと同時に，実験測定結果が示す垂直磁化現象を微視的に説明することに成功した。計算された MAE は，主に電子のスピン軌道相互作用および磁気双極子相互作用の２つに由来する。彼はこの２つの寄与を記憶層の膜厚依存性として求め，ある膜厚範囲に現れる垂直磁化の起源を，定量的に説明した。また MAE 電界制御係数と呼ばれる，電界に対する変化割合についても評価し，電界駆動型素子の開発に貢献した。彼の研究成果は，計算物質科学，ナノ科学，磁気デバイス開発等において重要である。

以上のような成果をまとめた本論文は，博士(理学)の学位に値するものと判定した。

４．審査結果　(1) 判　　定（いずれかに○印）　（合　格）・　不合格

(2) 授与学位　　博　士（　理学　）